GEOPHYSICS, VOL. 71, NO. 3 (MAY-JUNE 2006); P. G83–G91, 10 FIGS.
10.1190/1.2194900

Effects of spatially variable resolution on field-scale estimates of tracer concentration from electrical inversions using Archie's law

Kamini Singha[1] and Steven M. Gorelick[2]

ABSTRACT

Two important mechanisms affect our ability to estimate solute concentrations quantitatively from the inversion of field-scale electrical resistivity tomography (ERT) data: (1) the spatially variable physical processes that govern the flow of current as well as the variation of physical properties in space and (2) the overparameterization of inverse models, which requires the imposition of a smoothing constraint (regularization) to facilitate convergence of the inverse solution. Based on analyses of field and synthetic data, we find that the ability of ERT to recover the 3D shape and magnitudes of a migrating conductive target is spatially variable. Additionally, the application of Archie's law to tomograms from field ERT data produced solute concentrations that are consistently less than 10% of point measurements collected in the field and estimated from transport modeling. Estimates of concentration from ERT using Archie's law only fit measured solute concentrations if the apparent formation factor is varied with space and time and allowed to take on unreasonably high values. Our analysis suggests that the inability to find a single petrophysical relation in space and time between concentration and electrical resistivity is largely an effect of two properties of ERT surveys: (1) decreased sensitivity of ERT to detect the target plume with increasing distance from the electrodes and (2) the smoothing imprint of regularization used in inversion.

INTRODUCTION

Many studies have used electrical resistivity tomography (ERT) to monitor transient hydrogeologic processes and to estimate hydrogeologic-state variables such as water content and solute concentrations (Daily et al., 1992; Ramirez et al., 1993; Slater et al., 1997; Park, 1998; Ramirez and Daily, 2001; Zhou et al., 2001; Binley et al., 2002; Kemna et al., 2002; Yeh et al., 2002). However, using ERT data to quantitatively estimate these state variables in three dimensions remains an area of active research. One aspect of this research stems from the lack of information required to create predictive petrophysical relations between estimated bulk-media electrical resistivity and the variable of interest.

At the field scale, finding the correct petrophysical model is complicated by several issues:

1) the degree and spatial variability of subsurface conditions associated with aquifer heterogeneity;
2) the scarcity of colocated, directly monitored values for calibration to geophysical data or inversions;
3) the discrepancy in scale between lab measurements where petrophysical relations are often developed and the field-scale setting in which those relations are applied;
4) the decreased sensitivity of ERT with distance from the electrodes;
5) the effect of regularization on geophysical inversion and the choice of inverse parameterization; and
6) sensitivity as a function of the electrical-resistivity structure in the case of ERT; for time-varying processes such as solute migration, this last issue means that sensitivity is not only spatially variable but also temporally variable.

Because geophysical inverse problems are often underdetermined, given the limited amount of data that can be collected in the field, prior information about parameter correlation and the final model's appearance is often added via regularization. To remedy the ill-conditioned operator in the inverse problem, we use Tikhonov (1977) regularization, which biases the solution toward our a priori understanding of the appearance of the system and thereby stabilizes the inverse-problem formulation to yield a unique estimate of the geophysical parameter of interest. The subjective choice of how best to regularize affects the appearance of the tomogram as well as the consequent estimates and reliability of

Manuscript received by the Editor April 25, 2005; revised manuscript received August 10, 2005; published online May 22, 2006.
[1]Formerly Stanford University, Department of Geological and Environmental Sciences, Stanford, California 94305-2115; presently Pennsylvania State University, Department of Geosciences, University Park, Pennsylvania 16802. E-mail: ksingha@psu.edu.
[2]Stanford University, Department of Geological and Environmental Sciences, Stanford, California 94305-2115. E-mail: gorelick@pangea.stanford.edu.

the hydrogeologic variables calculated according to a petrophysical relation used to convert local resistivities into water contents or solute concentrations. Without accounting for the spatial variability in resolution when resolving inverted geophysical parameter values, estimating hydrogeologic variables from inverted tomograms using an empirical relation such as Archie's law (Archie, 1942) may have limited utility. However, without extensive hydrogeologic data, it is difficult to assess the performance of field-scale petrophysical calibrations.

Despite these problems, petrophysical relations such as Archie's law or other site-specific relations built from a few colocated data frequently continue to be used. Although Archie's law is a rough empirical approximation intended for a localized scale (e.g., the immediate vicinity of a wellbore), this empirical guideline has been accepted as a way to convert electrical-resistivity values to porosity when fluid resistivity is known. However, given the list of problems mentioned earlier, it is clear that field-scale relations between geophysical and hydrogeologic variables are site specific as well as survey and inversion specific.

In this work, we investigate the reliability of field-scale calibration in light of recent research on these issues (Day-Lewis and Lane, 2004; Moysey and Knight, 2004; Day-Lewis et al., 2005; Moysey et al., 2005). We show that estimating field-scale hydrogeologic-state variables from geophysical inversions may be difficult even when site-specific petrophysical relations are available.

FIELD EXPERIMENT

In a field experiment described in Singha and Gorelick (2005), ERT was used to monitor an unequal-strength doublet sodium chloride (NaCl) tracer test for 20 days at the U. S. Geological Survey's Toxic Substances Hydrology Program research site at the Massachusetts Military Reservation (MMR) on Cape Cod, Massachusetts (Figure 1). In an unequal-strength doublet tracer test, the injection and pumping rates are not the same. In this case, the pumping rate is three times the injection rate.

The aquifer is composed of glacial outwash — predominantly sand and gravel with less than 0.1% clay (Barber, 1987). The average hydraulic conductivity is approximately 110 m/day and ranges over the site by about one order of magnitude (Garabedian et al., 1991). The average effective porosity has been estimated to be between 0.28 and 0.39 (Garabedian et al., 1991; Singha and Gorelick, 2005).

The injection and pumping wells were 10 m apart, 26.5 m deep, fully screened, and surrounded by four ERT wells (Figure 2). The injection line within the injection well extended from 7.0 m to 22.2 m below ground surface (bgs). The four ERT wells were fully screened, 33.0 m deep, and instrumented with 24 ERT electrodes each. The injected tracer had an NaCl concentration of 2200mg/liter (470 mS/m), which was notably higher than the average background concentration of approximately 65 mg/liter (15 mS/m).

Freshwater with a concentration of approximately 12 mg/liter NaCl (2.4 mS/m) was injected into the aquifer before and after the 9-hour tracer-injection period. Tracer concentrations were measured 250 times during the 20-day doublet tracer test at a centrally located, 15-port multilevel sampler (Figure 3). Each multilevel sampler port was separated by 1.8 m, with the upper port at the water table located 5.5 m bgs and the bottom port at 31.1 m bgs. The injection rate throughout the test was 13.3 liters/minute, while the pumping rate was constant at 38.6 liters/minute. The initial hydraulic gradient prior to pumping was approximately 0.001.

ERT snapshots were collected every 6 hours during the 20-day test. For each ERT data set, 3150 unique resistance measurements were made using a circulating dipole-dipole scheme that included the following dipole configurations: (1) current and potential dipoles in the same well, (2) each dipole split between two wells, and (3) a mixed array where one dipole was split between two wells and the other was in the same well. Geometric factors for converting resistance to resistivity for these acquisition geometries ranged from approximately 6 to 580 m.

To minimize temporal smearing that would impact resultant tomograms, data collection was limited. The data had good reciprocal measurements, with noise less than 1% for most measurements. For each snapshot, data with reciprocal errors larger than 5% were removed from the data set prior to inversion; approximately 20 to 50 measurements of the 3150 collected were removed. For inversion, the model domain was discretized into nearly 150 000 elements in 3D. The inversion process is described below.

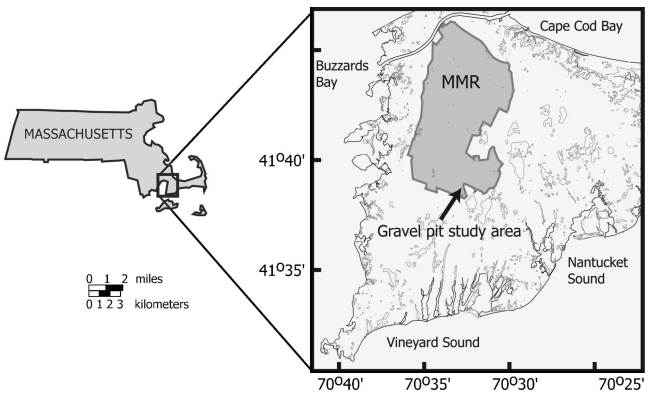

Figure 1. Location of the field site. The combined crosswell ERT and sodium chloride tracer experiment was conducted at the Massachusetts Military Reservation, Cape Cod, Massachusetts.

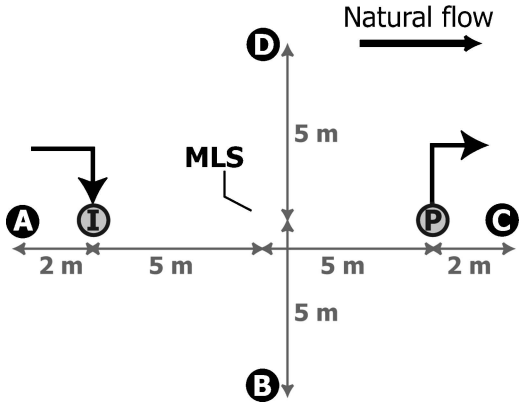

Figure 2. Geometry of well field in map view. ERT wells are labeled A-D. Injection and pumping wells are labeled I and P, respectively. The distance between ERT wells A and C is 14 m, and the distance between the ERT wells B and D is 10 m.

ERT INVERSION

Electrical flow is described by

$$A(m)\phi = q, \tag{1}$$

where $A(m)$ is the nonlinear operator describing the physics of the experiment, m are the model unknowns (in this case, the natural log of electrical resistivity), ϕ are the electrical potentials at each node, and q is the vector of current sources. Equation 1 describes a spatially diffusive process in which small-scale information is lost during data collection.

For each ERT snapshot data set, numerous resistance measurements, which are current-normalized changes in voltage, are collected. To invert the resistance data, we overparameterize the model space and find a single solution that minimizes the objective function with respect to the $L2$ norm using

$$\Omega = \|WR_{obs} - WR_{est}\|^2 + \beta\|Dm\|^2, \tag{2}$$

where W is a diagonal matrix used to weight individual resistances based on the variance of the measurements as described below, R_{obs} are the measured data (resistances) obtained in the field from ERT, R_{est} are the forward-model resistances, β is the regularization parameter that determines the importance given to the smooth appearance of the electrical-resistivity field relative to the misfit between calculated and observed resistance data, and D is a regularization matrix that in this study is based on a discretized 3D second-derivative operator, which enforces a smoothness constraint on the minimization function.

ERT inversions are affected by the sensitivity of the method and the effects of regularization. Inverted tomograms depend on the true distribution of electrical resistivities in the subsurface, as well as on how the resistance data were collected, as well as on how many and the geometry of the collected quadrupoles, how the model was parameterized, and how the regularization criteria were used in the inversion. Consequently, many solutions to the inverse problem exist. The solution to the objective function is generally found through a weighted least-squares formation of the inverse problem using iterative, gradient-based techniques (e.g., Daily et al., 1992; Ellis and Oldenburg, 1994; LaBrecque et al., 1996).

The ERT inversion routine used for this work is based on Occam's approach (Binley, personal communication, 2006). The final ERT tomogram is dependent on the assumed structure of the errors; resistivity contrasts in the subsurface and the occurrence in the inverted model and the occurrence of artifacts depend on how well the data are fit with respect to the assumed error model. At each iteration the inversion seeks to identify resistivity estimates that minimize the data misfit. This code uses an approach in which a target rms error is defined based on reciprocal measurements, as described in Binley et al. (1995). Being consistent with the underlying assumptions of using the $L2$ norm — i.e., that the data errors are randomly distributed — we assume the data residual between the normal and reciprocal measurements follow a Gaussian model. For this work we define our misfit tolerance ε according to error-variance model parameters a and b as

$$\varepsilon = a + b|R|, \tag{3}$$

where R is the measured resistance. For the field inversions, we use $a = 0.01$ ohms and $b = 0.05$ ohms. These values are determined by plotting reciprocal errors versus the measured resistances, as described in Slater et al. (2000), and calculating the slope and intercept of the envelope that encompasses the reliable data.

At each iteration of the inversion, a line search is performed to identify the β value that results in the lowest rms error not exceeding the target rms error, as defined by the misfit tolerance above (Kemna, 2000). The inversion continues until the rms error reaches the target rms error. The final result of the ERT inversion is a smooth 3D map of electrical resistivity (or, alternatively, conductivity) that best fits the resistance data to a given tolerance according to the parameterization.

For these field data, the recovered structure in the differenced ERT inversions are smooth and dispersed, which is common in tomograms reconstructed with a second-derivative filter. Differenced tomograms from field data show good sensitivity to changes in electrical resistivity associated with the movement of the tracer (Figure 4). Despite imaging the plume well, the ERT-estimated

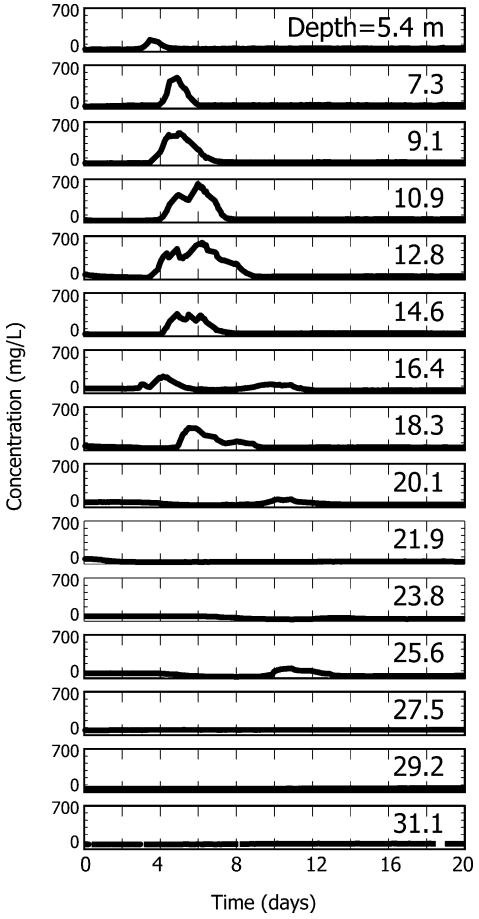

Figure 3. Sodium chloride concentration histories with depth. Each subplot corresponds to data from one of 15 ports on the centrally located multilevel sampler with depths labeled in meters and ranges from 0–700 mg/liter NaCl. First breakthrough occurred at the port situated 16.4 m below ground surface on day 3 after injection.

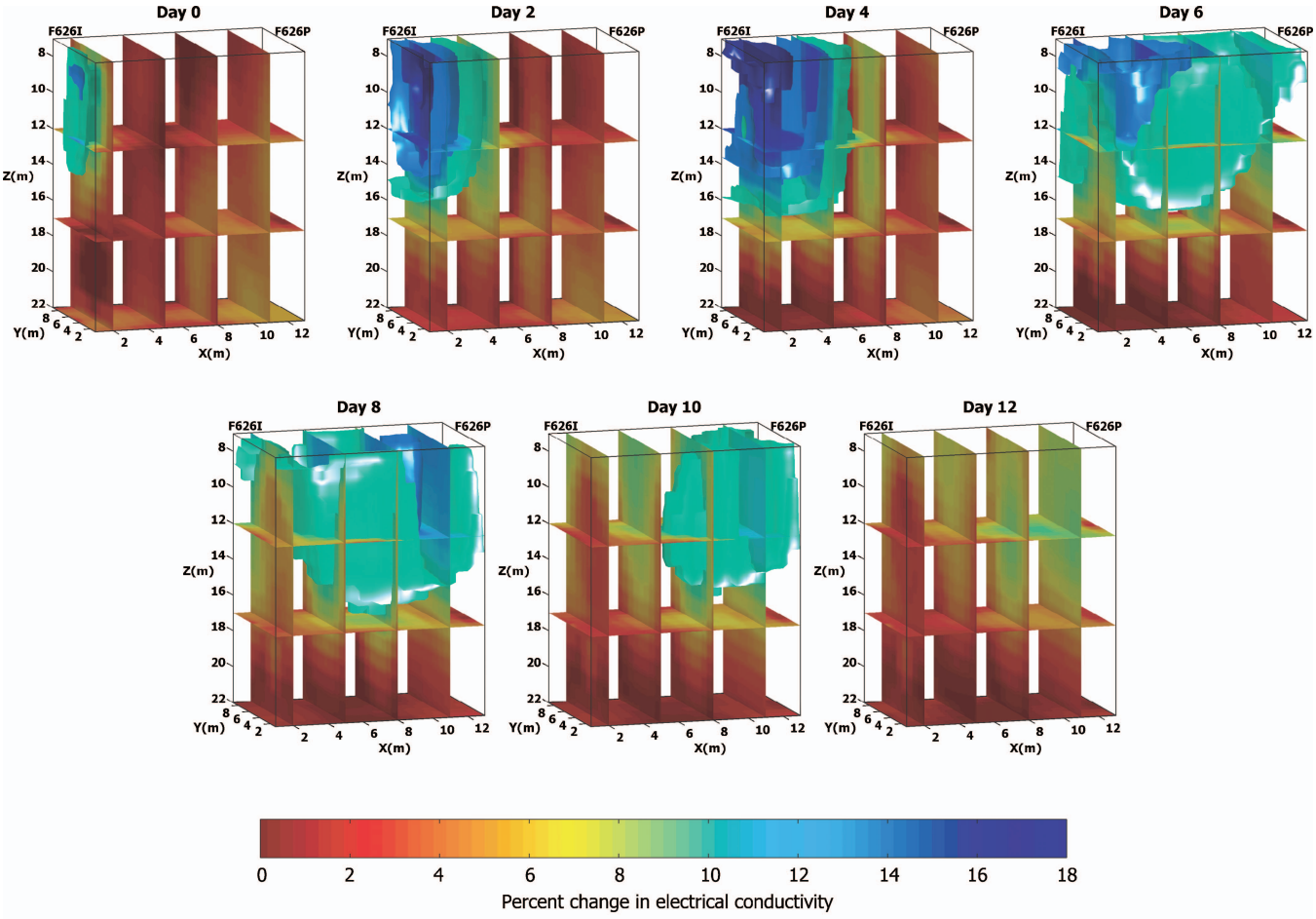

Figure 4. Snapshots from 3D tomograms indicating the percent change in electrical conductivity caused by the injected sodium chloride tracer compared to a background condition. Positive percent change in electrical conductivity (blue) indicates the presence of the tracer. Isosurfaces are at 10%, 14%, and 18% change.

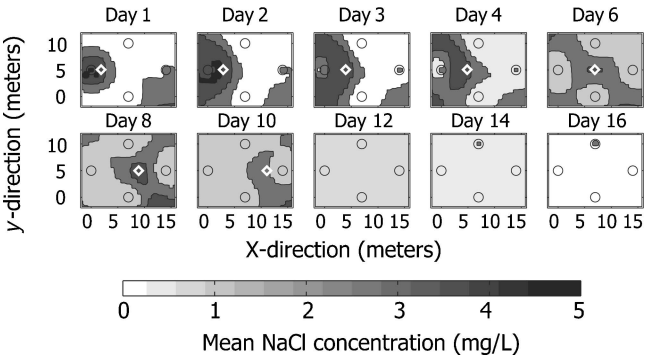

Figure 5. Average concentration through all layers of differenced 3D ERT inversions as calculated from the application of Archie's law, using a constant formation factor of five. ERT wells are shown as black circles (not to scale). As predicted by transport modeling, center of tracer mass is shown by white diamonds for days 1 through 10. Some anomalous values are apparent at the electrode locations.

concentration, as calculated given Archie's law and a site-specific calibration relation between fluid resistivity and concentration (Singha and Gorelick, 2005), is significantly lower than that measured in the aquifer. The data from the multilevel sampler show maximum concentrations as high as 700 mg/liter (Figure 3), whereas the maximum ERT estimate is less than 10 mg/liter (Figure 5), assuming a constant local formation factor of five, reasonable, given the high porosity sands at the field site, with Archie's law as follows:

$$\rho_b = F\rho_f, \tag{4}$$

where ρ_f is the fluid electrical resistivity measured at the multilevel sampler, ρ_b is the bulk-medium electrical resistivity measured by the ERT, and F is the formation factor associated with the porosity and tortuosity of the material originally defined as ϕ^{-m}, where ϕ is the porosity and m is the cementation exponent related to connectedness of pore space (Guyod, 1944), equal to approximately 1.3 for sands. We expect F to be between four and eight, given the porosity of the media at the site.

Other inversion decisions may produce different resistivity maps, but it is possible that none will match the true concentrations exactly. While the estimated electrical resistivity from the inver-

sion is only one of many possible solutions that would fit the measured resistance data, we are unlikely to recover the true subsurface resistivity and, consequently, the proper concentration magnitudes from ERT alone. We could create alternative models of resistivity that also match the data by making different regularization or parameterization choices; but an exact solution to the inverse problem exists only in continuous form when there is no noise in the data.

Errors are produced by discretization. Consequently, other maps of resistivity may match the directly measured values better; but no model of resistivity is likely to match the ground truth exactly, given the limited amount of data available for inversion in field studies. Stochastic inversion through Markov chain Monte Carlo methods can provide a better way to select resistivity maps that are most consistent with the data and a priori assumptions, as shown in Ramirez et al. (2005). However, these methods are still computationally intensive.

CALIBRATING ARCHIE'S LAW TO FIELD DATA

The goal of this work is to use ERT inversions to estimate spatially exhaustive concentration data quantitatively. However, it is clear that the ERT-estimated concentrations, using Archie's law, greatly underestimate the true concentrations seen in the field.

Given that the MMR site has very little clay, we can calculate the Archie's law formation factor (equation 4) that would fit the known fluid electrical resistivities (and consequently tracer concentrations) from direct sampling at the multilevel sampler, given the bulk-media electrical resistivities from the colocated ERT-inversion pixels. For every snapshot in time, the fluid resistivities from each fluid sample are divided into the colocated ERT-resistivity values to calculate the apparent formation factor. Temperature effects are negligible in this study.

Two results emerge from analysis using both the concentrations measured at the multilevel sampler and the colocated inverted ERT resistivities. First, to match the concentration data, we require apparent formation factors that lie beyond the range of values expected for these high-porosity unconsolidated sediments without clay (F = 4 to 8) at MMR. Second, and possibly more importantly, we find a formation factor that is a function which appears to vary with time (Figure 6). There is a distinct increase in the estimated formation factor from 4 to 20 during the period when the tracer passes by the multilevel sampler. We have identified three possible mechanisms that could produce these results, which are explored below.

Unresolved heterogeneity

Changes in the apparent formation factor through time have been seen in laboratory settings and have been attributed to different support volumes of the bulk and fluid measurements. Nonuniform salinity in the media at a support volume less than that of the ERT leads to variability in the Archie's law parameters with time (Knight and Endres, 2005). Although the volume captured by an electrical measurement (i.e., scale of support) is difficult to quantify (Daily and Ramirez, 1995), it averages over a much larger region than merely the volume of the fluid samples.

The samples collected in the field are 60 ml each. Assuming a porosity of 0.35, the sample volume is equivalent to a cube slightly larger than 5 cm on a side. Field-scale ERT cannot detect such detail. Although only suggestive of processes that might occur in the single-phase fluid problem, in multiphase systems such as oil and water or gas and water, it is well known that there is variability of fluid resistivity within the support scale of the ERT, since solute preferentially migrates through high-permeability regions. For multiphase systems this behavior is captured by Archie's second law for partial saturation (Archie, 1942).

Given that spatial variability in resistivity is a function of local salinity differences, a time-varying apparent formation factor would possibly suggest that local solute breakthrough occurs in a similar mixing relation for a single fluid phase. At early time the pore space is filled with nonsaline water, whereas at later time, when the tracer passes by the multilevel sampler between days five and nine, local aquifer heterogeneity causes partial filling of some pores with saltwater, while other local regions remain filled with nonsaline water. This is one possible explanation for the mismatch between the concentration samples and the ERT, which we revisit later.

Surface conductance

A second explanation for our observations of temporally variable formation factor is that we are dealing with dilute brines. The typical tracer salinities for this experiment are less than 5% of those of seawater, and the maximum NaCl concentration used in this test, 2200 mg/liter, is significantly more dilute than Archie's brines, which ranged from 20,000–100,000 mg/liter. The formation factor calculated from Archie's law assumes the existence of brine-saturated sediment, where ideally none of the solid material contributes to the electrical conduction. Therefore, the formation factor is defined only by pore geometry.

The apparent formation factor is affected by surface properties such as ionization of clay minerals and surface conductance. Surface conductance is dependent on the electrolyte concentration (Revil and Glover, 1997), and at low fluid electrical conductivities, it can be a significant issue. While numerous studies have documented an increase in formation factor with increasing concentra-

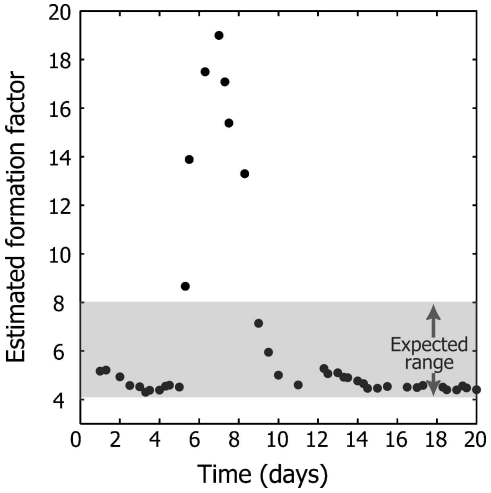

Figure 6. Formation factor estimated from colocated ERT and fluid samples at the multilevel sampler. Given a porosity of approximately 0.30 at the MMR field site, the true formation factor is estimated to be between four and eight, as indicated by the shaded area. The formation factor increases from a value of around five to approximately 20 during the period when the tracer passes by the multilevel sampler.

tion in diluted saline solutions (Patnode and Wyllie, 1950; Winsauer and McCardell, 1953; Waxman and Smits, 1968), surface conductance likely does not explain the change in apparent formation factor in our case. The sands at the field site have less than 0.1% clay (Barber, 1987) and a low cation-exchange capacity of approximately 0.53 meq/100 g (Ceazan et al., 1989). A Waxman-Smits adjustment for surface conductance, formulated in terms of electrical conductivities, is given by

$$\rho_b = \frac{1}{F}(BQ_v + \rho_f), \tag{5}$$

where ρ is the bulk-media resistivity measured by the ERT; ρ is the fluid electrical resistivity measured at the multilevel sampler; B is the counterion-equivalent conductance, which describes the average mobility of the ions; and Q_V is the counterion-charge concentration (meq/ml), which is directly related to the cation-exchange capacity.

Although many expressions have been developed to best estimate B (Mavko et al., 1998), Waxman-Smits defines it as

$$B = 4.6(1 - 0.6e^{-\rho_f/1.3}). \tag{6}$$

Given the small size of the cation exchange capacity, the BQ_v term changes by less than 15% and therefore cannot explain the misfit between the bulk and fluid electrical conductivities measured in the field.

Spatially variable resolution

A third explanation for the variation in formation factor is spatially and temporally varying sensitivity of the ERT to the presence of the tracer. The sensitivity is dependent on the subsurface resistivity, which changes over time because of the presence of an electrically conductive migrating tracer. Additionally, the inverted tomograms are smooth, so the change in the estimated bulk-media electrical resistivity will be small when compared to the changes in fluid resistivity that make the formation factor appear to vary.

Recent work by Day-Lewis et al. (2005) highlights that spatially variable resolution greatly impacts target recovery in geophysical tomograms and that ERT resolution is particularly poor in the center of the array. The current density is lowest away from the electrodes, so the sensitivity will also be the poorest in this location. According to equation 1 (electrical flow) is poorest in this location. The physics of measurement do not allow for ready detection of a target distant from the electrodes.

Given a simple target, such as a 1-ohm-m cylinder in a 100-ohm-m background (Figure 7), we find that the standard deviation of forward-modeled apparent resistivities decreases as the target moves away from the electrodes (Figure 8). Thus, with increasing distance from the electrodes, ERT is less sensitive to electrically conductive targets (Binley et al., 2002; Ramirez et al., 2003). Although only strictly the case when measurement error is Gaussian and uncorrelated, apparent resistivities within the range of 95–105 ohm-m may be indistinguishable from the background value of 100 ohm-m, given a measurement error of approximately 5% (shown as an error bar in Figure 8).

In-well dipoles, where both dipoles are in the same well, are most sensitive to the presence of the conductive cylinder. Cross-well dipoles, where the current and potential dipoles are each split between two wells, are least sensitive to the presence of the cylinder. In the presence of data noise when the target is distant from the electrodes and the distance between the target and source wells steadily increases, these measurements fall within the range of reasonable field noise, making the target nearly indistinguishable from the background.

These results suggest that when the target is distant from any of the wells — in this case, more than ~3.5 m — the primary information used to reconstruct the target reliably is contributed by the in-well dipole measurements. Of course, in similar field cases the particular distance value depends on the data-collection geometry used.

Coupled with spatial variability in measurement sensitivity is the effect of our choices of parameterization and regularization. The coupling of measurement insensitivity away from the electrodes and the effect of inversion on model-parameter values produces spatially variable resolution in the final ERT tomogram. To demonstrate these effects, we take a homogeneous cube with fluid resistivity equal to 40 ohm-m and assume a local constant formation factor of five, providing a true bulk resistivity over the cube of 200 ohm-m. However, given the same ERT geometry and inversion-model parameterization used in the field, the recovered resistivity values are not exactly 200 ohm-m but rather vary spatially from 184 to 202 ohm-m given a starting model of 185 ohm-m (Figure 9). These results are dependent on the geometry of the data-collection scheme and the number of data points collected as well as on the assumed error distribution. However, the results indicate that it is not always possible to recover a homogeneous system when using second-order Tikhonov regularization. Consequently, even in a homogeneous situation without uncaptured small-scale heterogeniety, the apparent formation factor may appear to vary in space solely as a function of spatially variable target recovery, discretization error, and choices associated with data inversion.

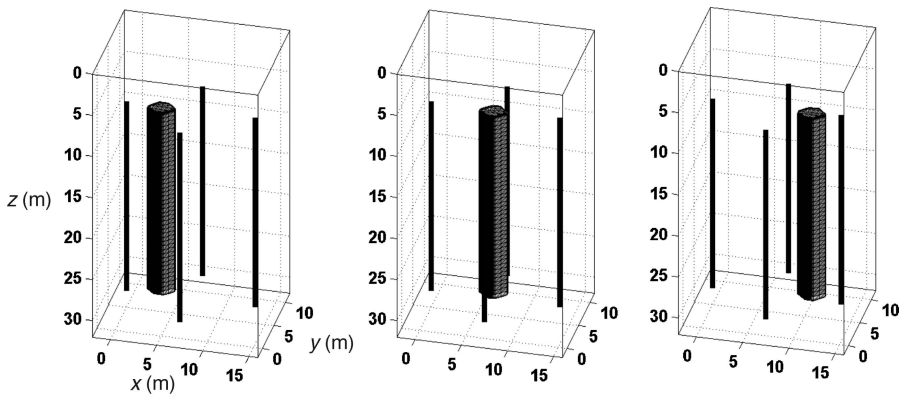

Figure 7. Geometry of ERT forward model considering the translation of a 1 ohm-m cylindrical target in a 100 ohm-m background. Wells are shown in map view as black lines with a long axis of 14 m and a short axis of 10 m.

While we could increase the degree of smoothing to correct this problem to some degree, this is not necessarily a

good general solution. In realistic problems, where heterogeneity is expected, oversmoothing may produce a larger data misfit than desired while obscuring structures present in the subsurface. The asymmetry in this figure is caused by slight asymmetry in the data collection geometry. The geometry was not symmetric because of the elimination of the quadrupoles with high reciprocal errors in the field. This geometry was used for this synthetic example.

EFFECT OF SPATIALLY VARIABLE RESOLUTION ON FIELD DATA

To explore the effect of spatially and temporally variable resolution on the field data, we create and explore a synthetic case that eliminates the physical effects of unresolved heterogeneity and surface conductance. Tracer migration and electrical flow were simulated for a simple example using the following procedure:

1) Develop a steady-state flow model (MODFLOW-96, Harbaugh and McDonald, 1996).
2) Develop a tracer-transport model (MT3DMS, Zheng and Wang, 1999).
3) Convert tracer concentration to local, bulk-media electrical resistivity following Archie's law.
4) Conduct forward geophysical simulation to synthesize ERT data.
5) Run a subsequent inverse model of the forward model resistances to estimate the 3D electrical-resistivity field.

For this exercise we simulate solute transport for a forced gradient tracer test, assuming a 2200-mg/liter solute source for 9 hours and collecting synthetic ERT snapshots daily for 20 days. We use a homogeneous hydraulic conductivity of 110 m/day and effective porosity of 0.32. The dispersivities are α_{11} = 0.1 m, α_{22} = 0.01 m, and α_{33} = 0.001 m, which best fit the concentration breakthrough data at the multilevel sampler and are used in this synthetic case as well. The longitudinal dispersivity α_{11} is one-tenth the interwell spacing — a reasonable estimate as shown in Gelhar et al. (1992). The synthetic-case geometry also mimics the field site, where the injection and pumping wells are 10 m apart and surrounded by four ERT wells (Figure 2). The synthetic tracer test mimics the field experiment in timing, concentration, and pumping rates.

Using the same geometry as in the field experiment for each ERT-snapshot data set, 3150 resistance measurements were collected. The inversion model was similarly parameterized and regularized to match the field case. The target data error level for synthetic inversions was based on 3% random noise added to the forward model resistances.

Application of Archie's law to the differenced inversion produces concentration estimates on the order of 5 mg/liter throughout the domain — clearly much less than the true concentration in the field produced by a 2200 -mg/liter injectate. If we consider simulated concentration data from a hypothetical, centrally located multilevel sampler, we find that a comparison of the concentrations from the transport model and colocated, inverted-ERT conductivities produce a time-

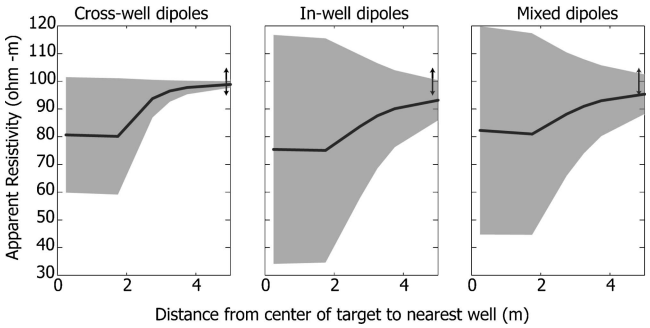

Figure 8. Mean of forward-modeled apparent resistivities for a 3D case where a 1-ohm-m cylinder located near an ERT well moves toward the center of the array. The 3150 measurements are separated by geometry type, including (1) crosswell dipoles where the current and potential dipoles are split between two separate wells (n = 1050); (2) in-well dipoles where current and potential dipoles are all in the same well (n = 756); and (3) a mixed array where one dipole is in one well and the other is split between two wells (n = 1344). The first standard deviation from the mean is shown in the gray envelope. The in-well dipoles are most sensitive to the presence of the cylinder at all locations in space, as indicated by the lowest mean apparent resistivity. The crosswell dipoles are least sensitive to the presence of the cylinder. For all geometries the variance in the measurements decreases as the cylinder increases its distance from the electrodes. In the presence of data noise, the cylinder may be difficult to detect in the center of the array. The black arrow represents 5% data noise from the background value of 100 ohm-m.

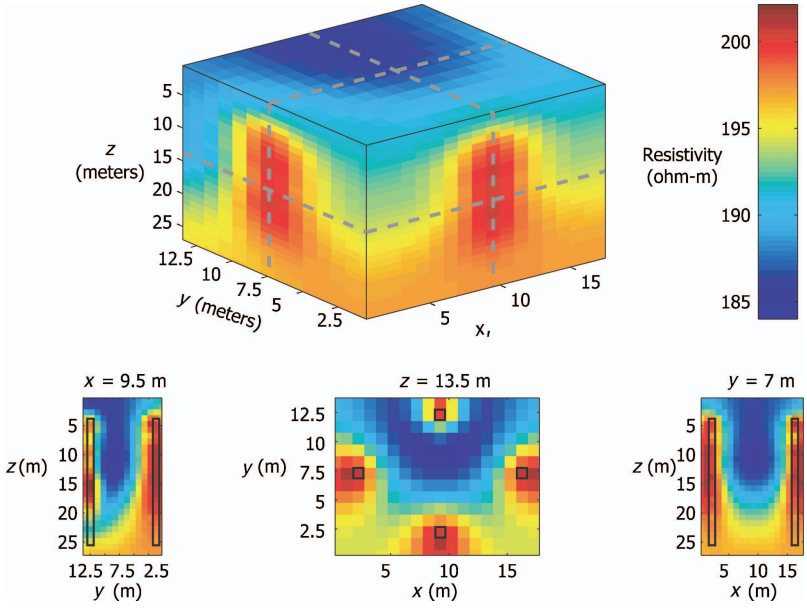

Figure 9. Spatially variable recovery of a homogeneous 200-ohm-m resistivity structure. The 3D tomogram is shown at the top and slices through the tomogram are shown below. Distances are in meters. Well locations are outlined in black. The tomogram values vary spatially because of decreased ability to recover targets with increasing distance from the electrode locations together with the regularization of the overparameterized inverse problem.

varying formation factor at any location (Figure 10).

Interestingly, variation in the depth-averaged formation factor resembles the time-varying, depth-averaged formation function that we see from analysis of our field data. In synthetic inversions the peak values of the formation factor range from 9.3-24.6 with depth (with a mean value of 19.0), and the average of the maximum-to-minimum values ranges from 4.6-12.3 with depth (with a mean value of 11.7). Based on field-data analysis at the multilevel-sampler location, the peak value of the formation factor is 14.3 and the average of the maximum-to-minimum values is 7.2, similar to those seen in the synthetic inversions. The high formation factors for these examples are caused in part by decreased ERT sensitivity away from the electrode locations. Additionally, the results show a decrease with time in formation factor because the tracer disperses during transport.

It is also particularly noteworthy that the apparent formation-factor values often exceed those expected when applying Archie's law to a homogeneous sand aquifer, which in this simulated case has no surface conductance. Just as significant, in this numerical experiment there is no subpixel mixing, and each pixel at any time has one distinct concentration. Thus, in this modeling exercise the change in apparent formation factor cannot be caused by nonuniform salinity in the pixel, described earlier as an effect of unaccounted heterogeneity. Additionally, the grid blocks used for the ERT and transport model are the same, so differing modeling scales also do not come into play.

Although the issues presented here are general in nature, the demonstration and severity of the problem are specific to the experimental design and inversion approach. Other experimental designs and inversion approaches, such as using $L1$ norms and other smoothing approaches, could reduce (although likely not eliminate) the magnitude of the problem. The effects of spatially variable sensitivity will plague most if not all studies. Consequently, the existing classical lab-scale rock physics relation will be unable to predict tracer concentrations from resistivity inversions.

The direct application of Archie's law does not describe the complexity of the field-scale relation between fluid resistivity and bulk-ERT resistivity because of spatially and temporally varying resolution, including measurement sensitivity and inversion effects such as smoothing resulting from regularization. We find that this problem exists without introducing effects of surface conductance or nonuniformity of the Archie parameters. Also, analysis of our field data suggests that we are able to reproduce the apparent formation factor with time. Because neither surface conductance nor scale was an element of the synthetic data, we contend that the variability in formation factor seen in the field case is caused principally by spatially variable resolution. These results suggest that spatial and temporal variability in tomogram resolution based on ERT inhibits accurate recovery of changes in bulk-media electrical resistivity away from the electrodes without invoking surface-conductance phenomena or without invoking surface-conductance or support-scale phenomena.

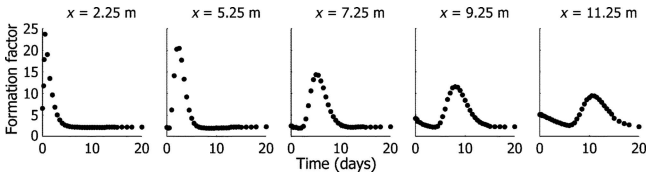

Figure 10. Formation factor versus time at selected locations parallel to flow along the centerline. Formation factors are generated based on a synthetic example from colocated values of ERT conductivities and fluid conductivity from an MT3DMS simulation. ERT wells are at $x = 0$ and $x = 14$ m. The multilevel sampler is located at $x = 7.25$ m. The true formation factor is five. As the tracer passes through selected locations, an apparent increase in the formation factor occurs because of poor ERT sensitivity, which underestimates the true bulk-media conductivity at the pixel scale when compared to the fluid conductivity from transport modeling.

Based on the results presented here, to accurately estimate fluid electrical resistivity and thereby tracer concentration from estimated bulk-media electrical resistivity, we must develop intelligent ways to parameterize the ERT inverse problem, such as using object-based inversion methods that have been demonstrated for crosswell radar methods (Lane et al., 2004), or we must consider a petrophysical relation that changes with space and time. However, building relations that change with space and time is difficult, given the extensive fluid-resistivity data required. Recently, Moysey et al. (2005) have developed a method based on numerical analogs via Monte Carlo simulation for building spatiotemporally varying relations for radar tomography for 2D synthetic work. Similar methods for ERT likely would improve estimates of tracer concentration from inverted electrical tomograms.

CONCLUSIONS

The use of a petrophysical relation to estimate tracer concentration from ERT should account for the spatial and temporal variability in the resolution of inverted tomograms. Two important mechanisms affect our ability to estimate hydrogeologic variables from ERT quantitatively: (1) the spatially and temporally variable physical processes that govern the flow of current through a migrating saline plume and (2) the overparameterization of the inverse models that requires the imposition of a smoothing constraint (regularization) to facilitate convergence of the inverse solution. Because these two mechanisms are spatially and temporally variable, the ability of ERT to recover the 3D shape and magnitudes of a migrating conductive target is similarly variable.

Given the variability in ERT sensitivity across the field site in space and time, any mathematical relation or statistical correlation built between colocated fluid and estimated bulk-media electrical conductivities at a particular location would not necessarily be appropriate elsewhere in the tomogram or even at the same location at another time. Our field data and numerical experiments suggest that the direct application of a petrophysical relation, in this case Archie's law, to obtain solute concentrations from bulk-media electrical-resistivity tomograms will produce misleading estimates of concentration. Most significantly, the Archie formation factor appears to change because of the varying spatiotemporal resolution of ERT during a two-well tracer test — either synthetic or based on field data. In past studies this has been attributed to nonuniform salinity below the measurement scale of the geophysics. We believe that in this case the issue of spatially variable resolution in tomograms is of key importance and should be considered in future studies. Finding methods to quantify concentration magnitudes or other hydrogeologic parameters accurately remains a research challenge.

A problem inherent in the quantitative use of geophysical data is the lack of information necessary to find a predictive petrophysical relation between the measured geophysical parameters in the field and the geologic or hydraulic parameters or state variables of inter-

est at this scale. Our work suggests that to build site-specific (as well as survey- and inversion-specific) relations for ERT, quanti fication of spatially variable resolution is required along with colocated measurements of concentration and estimated bulk-media resistivity. In this work, we contend that expecting any single petrophysical model to successfully transform electrical-tomography inversions into tracer concentrations may be difficult without survey-specific information about the relation between resistivity and tracer concentration. Field-scale relations between electrical resistivity and concentration must be site, survey, and inversion specific.

ACKNOWLEDGMENTS

The authors thank Andrew Binley of Lancaster University for the use of and instruction in his ERT inversion code. We gratefully acknowledge the advice and assistance for the field portion of this work provided by Denis LeBlanc, Kathy Hess, John W. Lane Jr., and Carole Johnson of the U. S. Geological Survey as well as the support from the USGS Toxic Substances Hydrology Program. This material is based upon work supported by the National Science Foundation under grant EAR-0124262. Any opinions, findings, and conclusions or recommendations expressed in this material are those of the authors and do not necessarily reflect the views of the National Science Foundation.

REFERENCES

Archie, G. E., 1942, The electrical resistivity log as an aid in determining some reservoir characteristics: Transactions of the American Institute of Mining, Metallurgical and Petroleum Engineers, **146**, 54–62.

Barber, L. B., 1987, Influence of geochemical heterogeneity in a sand and gravel aquifer on the transport of nonionic organic solutes — Methods of sediment characterization, in U. S. Geological Survey program on toxic waste — Ground-water contamination, B. J. Franks, ed., B45-B51. Proceedings of the Third Technical Meeting, U. S. Geological Survey Open-File Report 87-109.

Binley, A., G. Cassiani, R. Middleton, and P. Winship, 2002, Vadose zone flow model parameterisation using cross-borehole radar and resistivity imaging Journal of Hydrology, **267**, 147–159.

Binley A., A. Ramirez, and W. Daily, 1995, Regularised image reconstruction on noisy electrical resistance tomography data: 4th Workshop of the European Concerted Action on Process Tomograpgy, Proceedings, 401–410.

Ceazan, M. L., E. M. Thurman, and R. L. Smith, 1989, Retardation of ammonium and potassium transport through a contaminated sand and gravel aquifer: The role of cation exchange: Environmental Science & Technology, **23**, 1402–1408.

Daily, W., and A. Ramirez, 1995, Electrical resistance tomography during in-situ trichloroethylene remediation at the Savannah River site: Journal of Applied Geophysics, **33**, 239–249.

Daily, W., A. Ramirez, D. LaBrecque, and J. Nitao, 1992, Electrical resistivity tomography of vadose water movement: Water Resources Research, **28**, 1429–1442.

Day-Lewis, F. D., and J. W. Lane Jr., 2004, Assessing the resolution-dependent utility of tomograms for geostatistics: Geophysical Research Letters, **31**, L07503 doi:07510.01029/02004GL019617.

Day-Lewis, F. D., K. Singha, and A. M. Binley, 2005, Applying petrophysical models to radar traveltime and electrical-resistivity tomograms: Resolution-dependent limitations: Journal of Geophysical Research, **110**, B08206 doi:10.1029/2004JB003569.

Ellis, R. G., and D. W. Oldenburg, 1994, Applied geophysical inversion: Geophysical Journal International, **116**, 5–11.

Garabedian, S. P., D. R. LeBlanc, L. W. Gelhar, and M. A. Celia, 1991, Large-scale natural gradient tracer test in sand and gravel, Cape Cod, Massachusetts, 2, Analysis of spatial moments for a nonreactive tracer: Water Resources Research, **27**, 911–924.

Gelhar, L. W., C. Welty, and K. R. Rehfeldt, 1992, A critical review of data on field-scale dispersion in aquifers: Water Resources Research, **28**, 1955–1974.

Guyod, H., 1944, Fundamental data for the interpretation of electric logs: Oil Weekly, **115**, 21–27.

Harbaugh, A. W., and M. G. McDonald, 1996, User's documentation for MODFLOW-96, an update to the U. S. Geological Survey Modular Finite-Difference Ground-Water Flow Model: U. S. Geological Survey Open-File Report 96-485.

Kemna, A., 2000, Tomographic inversion of complex resistivity: Theory and application: Ph.D. dissertation, Ruhr University.

Kemna, A., J. Vanderborght, B. Kulessa, and H. Vereeken, 2002, Imaging and characterisation of subsurface solute transport using electrical resistivity tomography (ERT) and equivalent transport models: Journal of Hydrology, **267**, 125–146.

Knight, R. J. and A. L. Endres, 2005, Physical properties of near-surface materials and approaches to geophysical determination of properties, *in* D. Butler, ed., An introduction to rock physics for near-surface applications: SEG.

LaBrecque, D. J., M. Miletto, W. Daily, A. Ramirez, and E. Owen, 1996, The effects of noise on Occam's inversion of resistivity tomography data: Geophysics, **61**, 538–548.

Lane, J. W., Jr., F. D. Day-Lewis, R. J. Versteeg, and C. C. Casey, 2004, Object-based inversion of crosswell radar tomography data to monitor vegetable oil injection experiments: Journal of Environmental and Engineering Geophysics, **9**, 63–77.

Mavko, G., T. Mukerji, and J. Dvorkin, 1998, The rock physics handbook: Cambridge University Press.

Moysey, S., and R. J. Knight, 2004, Modeling the field-scale relationship between dielectric constant and water content in heterogeneous systems: Water Resources Research, **40**, W03510 doi:03510.01029/02003 WR002589.

Moysey, S., K. Singha, and R. Knight, 2005, A framework for inferring field-scale rock physics relationships through numerical simulation: Geophysical Research Letters, **32**, L08304 doi:08310.01029/02004GL 022152.

Park, S. K., 1998, Fluid migration in the vadose zone from 3-D inversion of resistivity monitoring data: Geophysics, **63**, 41–51.

Patnode, H. W., and M. R. J. Wyllie, 1950, The presence of conductive solids in reservoir rocks as a factor in electric log interpretation: Petroleum Transactions, The American Institute of Mining, Metallurgical, and Petroleum Engineers, **189**, 47–52.

Ramirez, A., and W. Daily, 2001, Electrical imaging at the large block test — Yucca Mountain, Nevada: Journal of Applied Geophysics, **46**, 85–100.

Ramirez, A., W. Daily, D. LaBrecque, E. Owen, and D. Chesnut, 1993, Monitoring an underground steam injection process using electrical resistance tomography Water Resources Research, **29**, 73–87.

Ramirez, A., R. Newmark, and W. Daily, 2003, Monitoring carbon dioxide floods using electrical resistance tomography (ERT): Sensitivity studies: Journal of Environmental and Engineering Geophysics, **8**, 187–208.

Ramirez, A. L., J. J. Nitao, W. G. Hanley, R. Aines, R. E. Glaser, S. K. Sengupta, K. M. Dyer, T. L. Hickling, and W. D. Daily, 2005, Stochastic inversion of electrical resistivity changes using a Markov chain Monte Carlo approach: Journal of Geophysical Research, **110**, B02101 doi:10.1029/2004JB003449.

Revil, A., and P. W. J. Grover, 1997, Theory of ionic surface electrical conduction in porous media: Physics Review, **B55**, 1757–1773.

Singha, K., and S. M. Gorelick, 2005, Saline tracer visualized with electrical resistivity tomography: field scale moment analysis: Water Resources Research, **41**, W05023 doi:05010.01029/02004WR003460.

Slater, L., A. M. Binley, W. Daily, and R. Johnson, 2000, Cross-hole electrical imaging of a controlled saline tracer injection: Journal of Applied Geophysics, **44**, 85–102.

Slater, L., M. D. Zaidman, A. M. Binley, and L. J. West, 1997, Electrical imaging of saline tracer migration for the investigation of unsaturated zone transport mechanisms: Hydrology and Earth System Sciences, **1**, 291–302.

Tikhonov, A. N., and V. Y. Arsenin, 1977, Solutions of ill-posed problems: John Wiley & Sons.

Waxman, M. H., and L. J. M. Smits, 1968, Electrical conductivities in oil-bearing shaly sands: Society Petroleum Engineers Journal, **8**, 107–122.

Winsauer, W. O., and W. M. McCardell, 1953, Ionic double-layer conductivity in reservoir rock: Petroleum Transactions, The American Institute of Mining, Metallurgical, and Petroleum Engineers, **198**, 129–134.

Yeh, T. C. J., S. Liu, R. J. Glass, K. Baker, J. R. Brainard, D. L. Alumbaugh, and D. LaBrecque, 2002, A geostatistically based inverse model for electrical resistivity surveys and its applications to vadose zone hydrology: Water Resources Research, **38**, 14–11–14–13.

Zheng, C., and P. P. Wang, 1999, MT3DMS: A modular three-dimensional multispecies model for simulation of advection, dispersion and chemical reactions of contaminants in groundwater systems — Documentation and user's guide: U. S. Army Engineer Research and Development Center.

Zhou, Q. Y., J. Shimada, and A. Sato, 2001, Three-dimensional spatial and temporal monitoring of soil water content using electrical resistivity tomography: Water Resources Research, **37**, 273–285.